EFFECTS OF WALL STIFFNESS ON THE LINEAR STABILITY OF FLOW IN AN ELASTIC CHANNEL

X. Y. Luo
Department of Mechanical Engineering, University of Sheffield, UK

Z.X. Cai
Department of Mechanics, Tianjin University, China

ABSTRACT

The aim of this paper is to explore the key influences of the wall stiffness on the stability and self-excited oscillations of the flow in collapsible channels. To identify mechanism of the oscillations found in the full numerical solutions, a linear eigenvalue problem of the Orr-Sommerfield equations modified by the beam is solved. Excellent agreement is found between the onset of small amplitude oscillations in the full numerical simulations and the neutral stability curves from the eigenvalue problem. If the neutral stability curve is shown in the dimensionless pre-tension and wall stiffness space, there appears to be a "stability zone" inside an unstable region as either the pre-tension is reduced, with the wall stiffness fixed, or the tension fixed, and the wall stiffness is reduced. Further investigation of this "stability zone" over a wider range of parameters led to the conclusion that the pre-tension and the wall stiffness of the beam do not play independent roles in the linear stability of the system. Instead, the final tension, which is brought about by a combination of the pre-tension, wall stiffness and wall deformation is found to be the dominant factor in this system. A physical explanation of the existence of this stability zone is, however, still lacking.

1. INTRODUCTION

Flow in collapsible tubes has been extensively studied in the last few decades not only for its relevance to physiological applications, but also because of the interesting fluid-structure interactions that occur (Shapiro,1977; Grotberg & Gavirely,1989; Kamm & Pedley, 1989; Jensen,1990; Davies & Carpenter, 1997ab; Heil,1997; Matsuzaki, 1995). Self-excited oscillations are frequently observed in a Starling resistor made from such a system in the laboratory (Bertram,1982; Bertram,1990). Such oscillations have also been obtained from certain one-dimensional models (Jensen,1990), as well as in a two-dimensional fluid-membrane model (Luo & Pedley, 1996) which may, in principle, be realized in a laboratory.

The fluid-membrane model, however, suffers from several *ad hoc* approximations: the extensional and bending wall stiffness was ignored, and the elastic wall was assumed to move either in the vertical or in the normal direction. Although these may be adequate for steady flow simulations, their influence on unsteady flows, especially on the self-excited oscillations, needs to be carefully evaluated.

This paper studies the stability of a new fluid-beam model in which the solid mechanics of the wall is taken into account. Stability of a plane channel flow between compliant walls has been studied previously by a number of people (Green & Ellen, 1972; Davies, 2003). However, most of these studies considered flow in a long, parallel-sided channel, so in the basic state the steady flow is unidirectional and the elastic walls are planar. This should be contrasted with the present case, in which the steady flow, from which the oscillations grow, involves a large deformation of the wall and separation of the flow. These same steady solutions are also used as the basic state steady solutions for a linear stability analysis. This allows us to compare the eigenvalues from that analysis with the frequencies obtained from the full numerical results. In addition, we are able to follow the oscillations from their linear onset to the non-linear large-amplitude stage.

2. THE FLUID-BEAM MODEL

2.1 The model configuration

The model consists of a steady flow in a channel in which a part of the upper wall is replaced by an elastic beam, see figure 1. The rigid channel has width D, a part of the upper wall with length L is replaced by a pre-stressed elastic beam subjected to an external pressure p_e.

L_u and L_d are the lengths of the upstream and downstream rigid part of the channel. Steady Poiseuille flow with average velocity U_0 is assumed at the entrance. The flow is incompressible and laminar, the fluid having density ρ and viscosity μ. The extensional and bending stiffness of the beam are EA and EJ respectively, where E is the Young's modulus, A is the cross-sectional area of the beam, and J is the bending moment. The pre-tension in the beam (caused by an initial stretch of the beam) is T and the density of the beam is ρ_m. Damping and rotational inertia of the beam are both neglected.

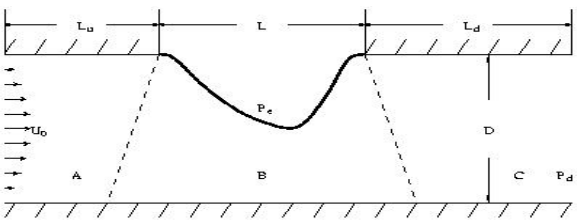

Figure 1: The flow-beam configuration (not to scale). Part B has part of the wall being replaced by an elastic beam.

2.2 The governing equations

For convenience, we introduce non-dimensionlized variables as follows:

$$u_i^* = \frac{u_i}{U_0}, \quad \sigma_i^* = \frac{\sigma_i}{\rho U_0^2}, \quad p^* = \frac{p}{\rho U_0^2}, \quad (i = 1,2)$$

$$T^* = \frac{T}{\rho U_0^2 D}, \; x^* = \frac{x}{D}, \quad y^* = \frac{y}{D},$$

$$t^* = \frac{tU_0}{D}, \; l^* = \frac{l}{D}, \; \kappa^* = \kappa D, \; \rho_m^* = \frac{\rho_m}{\rho D},$$

$$c_\lambda = \frac{EA}{\rho U_0^2 D}, \; c_\kappa = \frac{EJ}{\rho U_0^2 D^3}, \; \mathrm{Re} = \frac{U_0 D \rho}{\mu}$$

where variables with star are non-dimensional ones which will be used throughout this paper. In the following, however, the stars are dropped for simplicity.

The dimensionless governing equations for the system are thus: for the beam:

$$\frac{\rho_m}{\lambda}\left(x'\frac{d^2x}{dt^2} + y'\frac{d^2y}{dt^2}\right) = c_\kappa \kappa\kappa' + c_\lambda \lambda' + \lambda \tau_n = 0, \quad (1)$$

$$\frac{\rho_m}{\lambda}\left(y'\frac{d^2x}{dt^2} - x'\frac{d^2y}{dt^2}\right) = c_\kappa\left(\frac{1}{\lambda}\kappa'\right)' - \lambda\kappa T$$

$$-c_\lambda \lambda\kappa(\lambda - 1) - \lambda\sigma_n + \lambda p_e = 0, \quad (2)$$

$$x' = \lambda\cos\theta, \quad (3)$$

$$y' = \lambda\sin\theta \quad (4)$$

$$\theta' = \lambda\kappa \quad (5)$$

where the superscript ‘ denotes differentiation with respect to l. And for the fluid:

$$\frac{\partial u_i}{\partial t} + u_j u_{i,j} = -p_{,i} + \frac{1}{\mathrm{Re}} u_{i,jj}, \quad (6)$$

$$u_{i,i} = 0, \quad i, j = 1,2 \quad (7)$$

where the superscript prime represents derivative with respect to the initial beam position l. Notice that as both c_κ and $c_\lambda \to 0$, we recover the fluid-membrane model (Luo & Pedley, 1995). In this study, we choose $c_\lambda = 10^{-5} c_\kappa$ (i.e. the tube wall is thin).

Boundary conditions for the flow field are chosen such that steady parabolic velocity profile is used for the inlet flow, the stress free condition for the downstream outlet, and the no-slip condition is used along the walls including the elastic section. Clamped conditions are used for the beam ends.

3. NUMERICAL METHOD

A finite element code for unsteady flow is developed to solve the coupled nonlinear fluid-structure interactive equations simultaneously, and an adaptive mesh with rotating spines is used to allow for a movable boundary. The mesh is divided into three subdomains, one of which is placed with many spines originating from the bottom rigid wall to the movable beam, see figure 1.

These spines are straight lines, which can rotate around the fixed nodes at the bottom. Thus all the nodes on the spines can be stretched or compressed depending on the beam deformation. A numerical code is developed to solve the fluid and the beam equations simultaneously using weighted residual methods

A Petro-Galerkin method is used to discretise the system equations (1)-(7). The element type for flow is six-node triangular with second order shape function N_i for u and v, and linear shape function L_i for p. Three-node beam elements with second order shape function are used for x, y, θ, λ and κ. The discretized finite element equations can be written in a matrix form as

$$M(U)\frac{dU}{dt}+K(U)U-F=R=0 \qquad (8)$$

where $U=(u_j, v_j, p_j, x_j, y_j, \theta_j, \lambda_j, \kappa_j)$ is the global vector of unknowns, and j=1,…n, is the nodal number. R is the overall residual vector.

An implicit finite difference second order predictor-correct scheme with a variable time step is used to solve the time dependent problem. At each time step, the frontal method and a Newton-Raphson scheme are employed to obtain the converged solution for the whole system simultaneously.

4. LINEAR STABILITY ANALYSIS

As our numerical perturbations to the steady solutions are not strictly infinitesimal, we cannot say that the small amplitude oscillations are due to linear instability of the system. To investigate this, we now solve the eigenvalue problem of the linearized finite element equations, which is essentially the discretised Orr-Sommerfeld eigenvalue system, modified by the beam.

We denote the infinitesimal perturbation by ΔU, so that $U=\bar{U}+\Delta U$ is still a solution to the system. Here $\bar{U}$ is the steady solution obtained from the full numerical simulations. If the system is stable, then U should approach $\bar{U}$ as time increases. As in standard linear stability analysis, ΔU can be written in the form $\Delta\bar{U}=e^{\omega t}\tilde{U}$. Substituting this into (8) we obtain a matrix eigenvalue equation for the complex eigenvalues ω and eigenvectors $\tilde{U}$:

$$(\omega\bar{M}+\bar{K})\tilde{U}=\tilde{R}=0 \qquad (9)$$

where the matrices with a bar are determined by the steady solution $\bar{U}$. The eigenvalue matrix equation (9) is solved by using a QZ algorithm. The neutral stability curves obtained from solving (9) are shown in figure 2. It can be seen that the results from the stability analysis are in excellent agreement with the small amplitude oscillations calculated numerically. The points marked as S1, S2... came from the full numerical solutions discussed earlier, and they are all located extremely close to the neutral stability curves. The frequencies of these small amplitude oscillations also agree very well with the linear stability prediction.

In general, all the unstable solutions are located below the neutral curve I. This makes sense, as the system

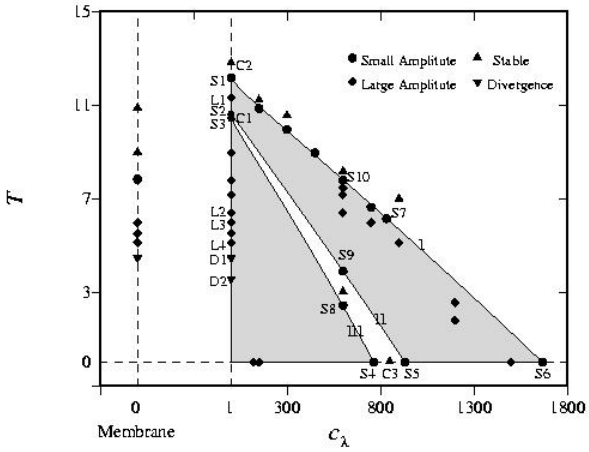

Figure 2 The neutral stability curve obtained from the eigenvalue solution. The shaded areas are unstable regions, and the white area is steady region.

tends to be more unstable for smaller tension or wall stiffness. What seems to be surprising is that inside this area there is a band of stable solutions. This stable band divides the unstable area into two regions, the upper unstable region and the lower one. For comparison, results for the corresponding membrane model are also shown in figure 2.

We notice that the small amplitude oscillations have roughly the same frequency if they are located on the same neutral stability curve. All these instabilities are, without exception, caused by mode 2 oscillations, each with a wavelength of one. The wall shapes of the solutions along each of the three curves are extremely similar to each other.

5. DISCUSSION

Figure 2 poses two interesting questions: why does a re-stability zone exist in the T- c_λ space? And why is there a frequency coincidence for oscillations with very different wall structural properties? Here we will make an attempt to answer these questions. Let us first examine the effects of T and c_λ for a wider Reynolds number range. The corresponding neutral stability curve for Re=1-600 are shown in figure 3. Again, we note that all the neutral stability points are mode-2 oscillations. On the left hand side of the curve, all the solutions are stable, on the right hand side of the curve, the solutions are unstable. Thus for this set of wall properties, the flow seems to reach its first neutral instability at about Re=200, and all solutions are unstable for Re beyond 500.

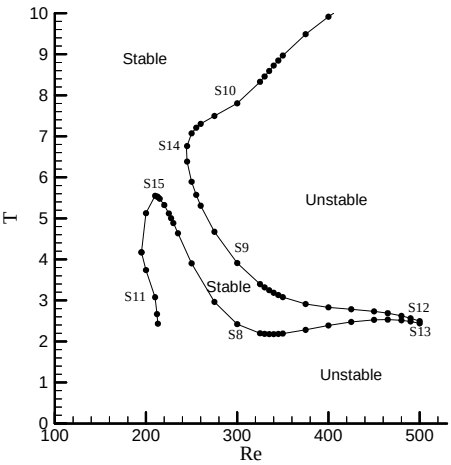

Figure 3 Neutral stability curve of mode-2 in the T- Re space for c_λ=600.

Figure 3 shows that the ``stability zone" observed in figure 2 is a manifestation of the stable tongue in the convoluted mode-2 stability curve; note the points S8, S9, S10 in both figure 3 and figure 2. The corresponding T-Re plot for $c_\lambda=1$ (not shown) is not convoluted and does not have a stable tongue; this is consistent with figure 2. Such a tongue is also absent for $c_\lambda=932.5$, as expected from figure 2. Thus the unexpected behaviour is not seen when the beam behaves like a membrane dominated by pre-tension T (c_λ very small) or when its extensional (or bending) stiffness c_λ is dominant. For the stable tongue to be seen both pre-tension T and stretching (or bending, since c_κ is proportional to c_λ) must play a role. We may also note that interactions between modes of different wave number, as found by Jensen (1990) in a one-dimensional model, are excluded, since only mode-2 oscillations are observed here.

Physical interpretation of these findings is not straightforward, especially when we recall that the non-dimensionalisation of pre-tension means that T is proportional to Re^2. However, we can say that there is no correlation between the development of instability and the occurrence of flow separation downstream of the elastic section. The latter occurs whenever the deformation is large, except at the lowest values of the Reynolds number (e.g. it does occur between S8 and S9 at Re=300, but not for some points to the right of S11 in figure 3).

Since flow separation is not crucial to instability, it may be instructive to compare our results with earlier work addressing the relative effects of bending stiffness and membrane tension in flow-induced instability of a compliant channel with walls that are initially planar, not deformed as in our case (Davies & Carpenter, 1997b). Their work suggests that the important structural properties which determine the system stability are tension and bending stiffness (the spring element in their model is absent here) for a massless wall. Using our non-dimensional variables, their theory predicted that oscillation will occur with frequency:

$$f = \frac{n(5TL^2 + 20c_\kappa n^2 - 3L^2)}{\sqrt{(10TL^2 + 40c_\kappa n^2 - L^2)}}. \qquad (10)$$

Note that c_λ does not appear since the membrane tension is supposed to be large enough not to change during small amplitude oscillations. However, it is important to recognise that T in (10) is different from our tension, since the value of T of Davies & Carpenter refers to the total membrane tension, while we use the pre-tension of the beam, not the actual tension in the steady state. The difference between these two definitions is negligible only when the wall deformation is small. The concept of the final tension, defined as

$$T_{final} = T + c_\lambda(\lambda - 1), \qquad (11)$$

has been discussed in detail by Cai & Luo (2003). In order to make quantitative comparison with Davies & Carpenter's theory, we need to estimate the "equivalent membrane tension" (or the final tension) from our beam model. Since the principal stretch λ varies along the beam, we estimate the final tension by calculating λ at a fixed station along the beam. The estimated final tension is plotted in figure 4. It is interesting to see that this curve is different from figure 3. The "stable tongue" has shrunk, and the slopes of its boundaries are positive, not negative. Aspect of this curve can be explained by looking at the ratio of the stretch-induced tension $c_\lambda(\lambda - 1)$, and the pre-tension, as shown in figure 5.

It can be seen that this ratio for the branches of the neutral curve running through S14 to S10, and through S15 to S11, is below unity, i.e., in these cases the pre-tension is greater than the stretch-induced tension. However, the ratio is much greater than one on the other two branches starting from S14 and S15, respectively, corresponding to a much greater wall deformation. It is worth pointing out that the stretch-induced tension in the branch passing through S8 is greater than in that passing through S9, which somewhat compensates for the fact that the pre-tension in the S9 branch is greater. The overall effect is thus to bring the gap between the two branches closer to each other in figure 4.

Using the estimated final tension to calculate the frequencies from (10) , we obtain the frequencies of the neutrally stable oscillations according to Davies & Carpenter's membrane model. The corresponding mode-

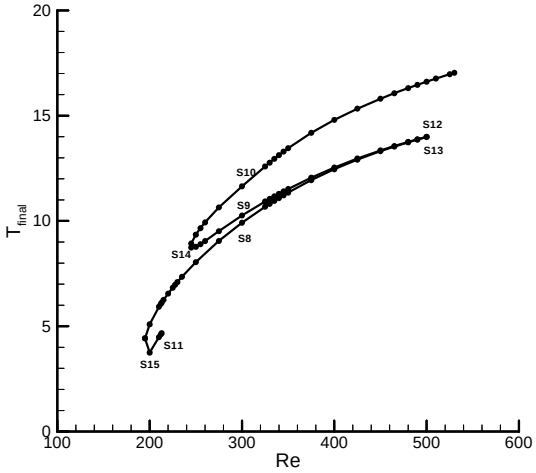

Figure 4 The neutral stability plotted as the final tension.

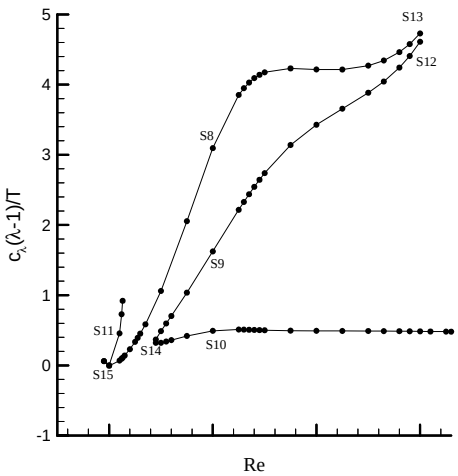

Figure 5 The neutral stability curve plotted as the ratio of the stretch induced tension with the pre-tension.

2 frequencies of our neutrally stable solutions are also computed. The results are shown in figure 6. It is highly interesting to see that their model gives a neutral curve with qualitatively similar shape to ours. However, the "stability zone" between S8 and S9 is even narrower accordingly to their model. This is confirmed by our further calculations of the neutral stability curve for $c\lambda=1$, where membrane effect is dominant, and no stable tongue was revealed.

Interestingly, predictions from even simpler linear stability theories for a stretched membrane with or without mean flow (Eq.(17) and (19) in Luo & Pedley, 1998, respectively) also indicated the same features: i.e.,

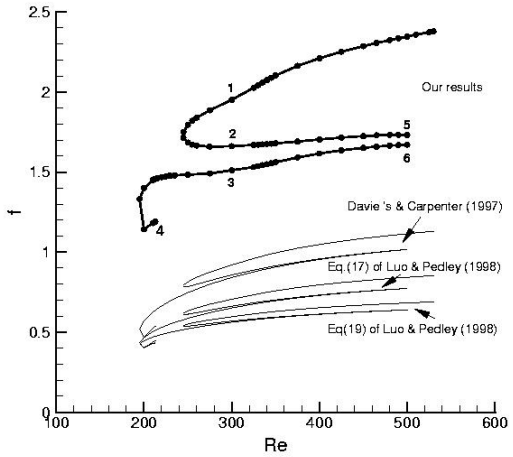

Figure 6 Comparison of the frequency calculated from our results and the previous linear theories.

there is still a narrow stable tongue, in a curve of similar shape: see figure 6. This strongly suggests that the final tension, be it the membrane tension, or the beam tension caused by the combination of pre-tension and wall stretch, is the dominant factor in the stability mechanism of this system. Of course, in the beam model, this final tension is not known *a priori*, and its precise value depends on the solution of a large-deformation fluid-structure interaction problem. Hence, unless for a small wall deformation (as assumed by most of the linear stability analyses), this key control parameter cannot be easily estimated from a beam model.

We may now explain the frequency coincidence on the three neutral stability curves in figure 2. The reason for the wall shapes to be similar along each of the curves can also be explained. It is interesting to note that, the way the wall moves in the x or y direction does not seems to have a significant influence on the linear stability of the system, as long as the amplitude of the wall oscillation is small.

In addition we have found that whether c_λ is chosen equal to 1 or 1667 in Davies and Carpenter's theory (with $c_\kappa=10^{-5}\ c_\lambda$) makes virtually no difference to the frequency predicted. Only when c_κ is several order of magnitude larger (implying a much thicker wall), do we observe some small difference in frequencies between $c_\lambda=1$ and 1667. Our conclusion is thus that for a thin walled channel, bending stiffness has a negligible effect on the linear stability of the system.

Since we only observed mode 2 oscillations in our computations, we know there could not be interactions from higher modes as was observed by Jensen (1990). However, even for the same mode, it is possible to find a mode interaction between a Tollimien-Schlichting wave and a flutter or a travelling-wave flutter, such a mode

interaction has been identified by Davies & Carpenter (1997b) and further elaborated by Davies (2003. It is possible that the narrow tongue presented in the f - Re plot is a result of such interactions. However, to identify the interactions in detail, further work is clearly needed.

6. CONCLUSION

Instability in a fluid-beam model has been studied in this paper. The most intriguing result from this study is the presence of a narrow tongue region when the neutral frequency is plotted against Reynolds number, where a stable zone is sandwiched by the unstable ones. We have found that such a narrow tongue can be qualitatively reproduced by linear theories for a tensioned membrane (Luo & Pedley, 1998) or fluid induced surface waves (Davies & Carpenter, 1997b; Davies:2003), if the final tension of the beam is used to calculate the frequency of the neutral stability. This seems to suggest that although the wall stiffness plays an important role in the unsteady behaviour of the system, it does so mainly by changing the final tension of the beam, and not by introducing a different mechanism. In other words, there is a strong indication that the final tension resulted from the pre-stretch, the stretching stiffness, and the wall shape plays the most important role in the linear stability of the system. However, the physical meaning for the narrow tongue to appear in the final tension of the beam model still remains unclear.

7. REFERENCES

Bertram, C. D., 1982, Two modes of instability in a thick-walled collapsible tube conveying a flow, *Journal of Biomechanics*, 15, 223-224.

Bertram, C. D. and Raymond, C. J. and Pedley, T. J., 1990, Mapping of instabilities for flow through collapsed tubes of differing length, *Journal of Fluid and Structures*, 4, 125-153.

Cai, Z.X., Luo X.Y., 2003, A fluid-beam model for flow in collapsible channel. *J. of Fluids and Structures* **17**, 123-144.

Davies, C. 2003, Convective and absolute instabilities of flows over compliant walls, Flow past Highly Compliant Boundaries and in Collapsible Tubes, *eds. P.W. Carpenter & T.J. Pedley, Kluwer Academic Publishers*, Dordrecht, The Netherlands. 69-94.

Davies, C. , Carptenter, P.W., 1997a, Instabilities in a plane channel flow between compliant walls. *J. of Fluid Mechanics*, 335, 205-243.

Davies, C. , Carptenter, P.W., 1997b, Numerical simulation of the evolution of Tollmien-Schlichting waves over finite compliant panels. *J. of Fluid Mechanics*, 335, 361-392.

Green, C. H. and Ellen, C. H., 192, he stability of plane Poiseuille flow between flexible walls, Journal *of Fluid Mechanics*, 51, 403-416.

Grotberg, J. B. and Gavriely, N., 1989, Flutter in collapsible tubes: a theoretical model of wheezes, *J. of Appl. Physiol*., 66, 2262-2273.

Heil, M., 1997, Stokes flow in collapsible tubes: computation and experiment, Journal of Fluid Mechanics, 353, 285-312.

Kamm, R.D. and Pedley, T. J., 1989, Flow in collapsible tubes: A brief review, *Trans. ASME, J. Biomech. Engng*. 11, 177-179,

Jensen, O.E., 1990 Instabilites of flow in a collapsed tube, *J. of Fluid Mechanics*, 220, 623-659.

Matsuzaki, Y. and Fujimura, K., 1995, Reexamination of steady solutions of a collapsible channelconveying fluid, A technical brief, *Trans. ASME, Journal of Biomech. Engng*, 117, 492-494.

Luo, X. Y. and Pedley, T. J., 1998, The effects of wall inertia on flow in a 2-D collapsible channel, *Journal of Fluid Mechanics*, 363, 253-280.

Luo, X. Y. & Pedley T. J., 1996, A numerical simulation of unsteady flow in a 2-D collapsible channel. *J. of Fluid Mechanics* **314,** 191-225.

Luo, X. Y., Pedley T. J., 1995, A numerical simulation of steady flow in a 2-D collapsible channel. *J. of Fluids & Structures*, **9**, 149-174.

Shapiro, A.H., 1977, Steady flow in collapsible tubes, *Trans. ASME, Journal of Biomechanical Engineering*, 99, 126-147.